Biochem. J. (1974) **139**, 321–329
Printed in Great Britain

Pig Liver Pyruvate Carboxylase

THE REACTION PATHWAY FOR THE DECARBOXYLATION OF OXALOACETATE

By GRAHAM B. WARREN* and KEITH F. TIPTON
Department of Biochemistry, University of Cambridge, Tennis Court Road, Cambridge CB2 1QW, U.K.

(*Received* 27 *September* 1973)

1. The reaction pathway for the decarboxylation of oxaloacetate, catalysed by pig liver pyruvate carboxylase, was studied in the presence of saturating concentrations of K^+ and acetyl-CoA. 2. Free Mg^{2+} binds to the enzyme in an equilibrium fashion and remains bound during all further catalytic cycles. $MgADP^-$ and P_i bind randomly, at equilibrium, followed by the binding of oxaloacetate. Pyruvate is released before the ordered steady-state release of HCO_3^- and $MgATP^{2-}$. 3. These results are entirely consistent with studies on the carboxylation of pyruvate presented in the preceding paper (Warren & Tipton, 1974*b*) and together they allow a quantitative description of the reaction mechanism of pig liver pyruvate carboxylase. 4. In the absence of other substrates of the back reaction pig liver pyruvate carboxylase will decarboxylate oxaloacetate in a manner that is not inhibited by avidin. 5. Reciprocal plots involving oxaloacetate are non-linear curves, which suggest a negatively co-operative interaction between this substrate and the enzyme.

Pig liver pyruvate carboxylase has been purified to homogeneity and the reaction pathway for the carboxylation of pyruvate has been elucidated as described in the two preceding papers (Warren & Tipton, 1974*a*,*b*). The present paper seeks to delineate the pathway for the decarboxylation of oxaloacetate in an effort to quantify the complete reaction pathway of the pig liver enzyme. These studies were performed at saturating concentrations of K^+ (110mM, K_m for K^+ = 20mM) and acetyl-CoA (100μM, K_s for acetyl-CoA = 22μM).

Materials

Pyruvate carboxylase, coupling enzymes and other assay components were obtained in the manner described in the two preceding papers (Warren & Tipton, 1974*a*, *b*).

Methods

Assays for pyruvate carboxylase

The enzyme was assayed in the back reaction by using a coupled assay for ATP (the ATP-coupled assay). The assay system contained 100mM-triethanolamine hydrochloride–KOH buffer, pH8.0, 0.5mM-ADP (0.36mM-$MgADP^-$), 10mM-P_i, 3.36mM-$MgSO_4$ (2.0mM-Mg^{2+}_{free}), 1mM-oxaloacetic acid, 0.1mM-acetyl-CoA, 2.5mM-glucose, 0.2mM-$NADP^+$, 25 units of hexokinase and 3 units of glucose 6-phosphate dehydrogenase in a total volume of 1.0ml at 30°C. The reaction was started by the addition of 50–120μg of pyruvate carboxylase, and the coupling-time required before the rate of $NADP^+$ reduction reached 99% of the steady-state rate of decarboxylation of oxaloacetate was approx. 35s (see McClure, 1969). The I of the medium was maintained at 200 $\pm$20mM by the addition of 1M-KCl, and variation within these limits had little effect on the rate of the enzymic reaction. The rate of reaction was monitored at 340nm except when kinetic studies were carried out at subsaturating concentrations of oxaloacetate. Since the K_m of the pig liver enzyme for this substrate was very low, the reaction was monitored at 366nm by using an Eppendorf fluorimeter.

When $MgATP^{2-}$ was used as a product inhibitor, pyruvate carboxylase was assayed by using a coupled assay for pyruvate (the pyruvate-coupled assay). The assay medium, in a total volume of 1.0ml, contained 100mM-triethanolamine hydrochloride–KOH buffer, pH8.0, 0.5mM-ADP (0.36mM-$MgADP^-$), 10mM-P_i, 3.36mM-$MgSO_4$ (2.0mM-Mg^{2+}_{free}), 0.1mM-oxaloacetic acid, 0.1mM-acetyl-CoA, 0.1mM-NADH and 11 units of lactate dehydrogenase. The reaction was started by the addition of 50–120μg of pyruvate carboxylase and the coupling time was 6s. Corrections were applied for the spontaneous decarboxylation of oxaloacetate (in the absence of pyruvate carboxylase) and the I was maintained at 200$\pm$20mM by the addition of 1M-KCl.

Studies on the decarboxylation of oxaloacetate alone, catalysed by pig liver pyruvate carboxylase, were carried out in a medium containing 100mM-triethanolamine hydrochloride–KOH buffer, pH8.0,

* Present address: National Institute for Medical Research, Mill Hill, London NW7 1AA, U.K.

90mM-KCl, 0.1mM-NADH, 11 units of lactate dehydrogenase and 0–0.1mM-oxaloacetate in a total volume of 1.0ml at 30°C. Reaction rates were monitored in the presence and absence of pyruvate carboxylase at 366nm by using an Eppendorf fluorimeter.

The specific activity of pyruvate carboxylase quoted in the Figure legends was derived by using the ATP-coupled assay and correcting for the subsaturating concentration of P_i. Kinetic results were plotted by the method of Lineweaver & Burk (1934) and the kinetic constants were evaluated by the method of Florini & Vestling (1957). K_i values were determined by the method of Dixon (1953).

Stability constants for the magnesium complexes of assay components

These were presented in the preceding paper (Warren & Tipton, 1974*b*) and were found to be little affected by the higher I value (200mM instead of 150mM) used in studies of the back reaction.

All other methods used in the present paper are described in the two preceding papers (Warren & Tipton, 1974*a*, *b*).

Results

Decarboxylation of oxaloacetate catalysed by pyruvate carboxylase

Pig liver pyruvate carboxylase significantly stimulated the decarboxylation of oxaloacetate in the absence of all other components of the back reaction. Low concentrations of kinetically contaminating enzymes (present in pure preparations of pyruvate carboxylase) such as malate dehydrogenase were not responsible for this effect and inactivation of pyruvate carboxylase with acid or alkali inhibited the reaction. Other enzymes capable of binding oxaloacetate, such as aspartate aminotransferase and citrate synthase, were also found to decarboxylate oxaloacetate. Since oxalate inhibited the decarboxylation catalysed by pyruvate carboxylase, the reaction appeared to be taking place at the α-keto acid-binding site. The K_m for oxaloacetate was 20μM and the V for decarboxylation was 55% of the V for the back reaction. However, in the presence of all of the other reaction components of the back reaction, the decarboxylation of oxaloacetate was completely coupled to the synthesis of $MgATP^{2-}$ from $MgADP^-$ and P_i. This was demonstrated during kinetic studies by using the pyruvate-coupled assay, since the reaction rate in the absence of pyruvate carboxylase was subtractable from rates obtained in the presence of the enzyme to yield linear reciprocal plots (Figs. 9 and 10).

Inactivation of pig liver pyruvate carboxylase with avidin did not inhibit the decarboxylation of oxaloacetate, although the K_m value was increased to 40μM. These results are qualitatively similar to those obtained by Scrutton & Mildvan (1968) for the chicken liver enzyme, although the rates of decarboxylation in the presence and absence of avidin were considerably lower in the latter case (approx. 0.3% of the V of the back reaction). Decarboxylation reactions have also been noted for other biotin carboxylases (Moss & Lane, 1972).

Kinetic studies using oxaloacetate

Reciprocal plots involving oxaloacetate yielded downwardly curving lines (Fig. 1) and the value of the Hill coefficient was not grossly affected by high concentrations of acetyl-CoA or 'infinite' concentrations of free Mg^{2+}, $MgADP^-$ or P_i (Table 1). The

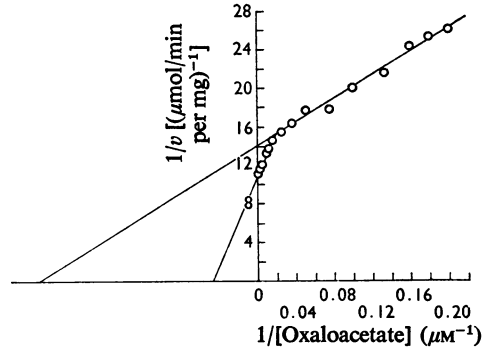

Fig. 1. *Reciprocal plot for the decarboxylation of oxaloacetate by pyruvate carboxylase*

Pyruvate carboxylase (90μg; 0.16 units/mg) was added to the ATP-coupled assay. The high and low K_m values determined by extrapolation of the linear portions of the plot were 22μM and 4.3μM respectively.

Table 1. *Hill coefficients for oxaloacetate*

Conditions refer to the concentrations of the back reaction components in the ATP-coupled assay unless as stated below. The value for the Hill coefficient at an 'infinite' concentration of a back reaction component was evaluated from the intercept replot of a primary plot involving the back reaction component at several fixed concentrations of oxaloacetate.

Condition	Hill coefficient
—	0.67
0.5mM-Acetyl-CoA	0.65
'Infinite' free Mg^{2+}	0.60
'Infinite' $MgADP^-$	0.42
'Infinite' P_i	0.50

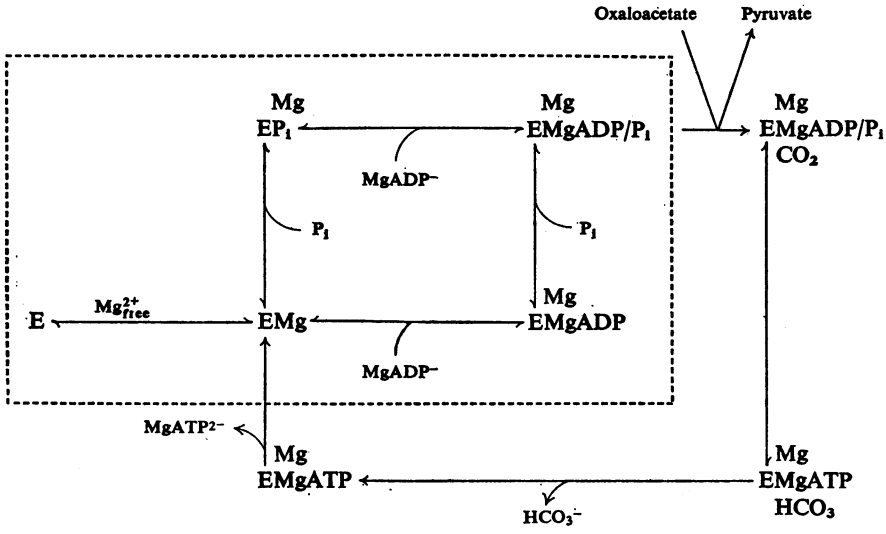

Scheme 1. *Reaction pathway for the decarboxylation of oxaloacetate by pig liver pyruvate carboxylase*

The section enclosed within the broken line is in rapid equilibrium, and E_{CO_2} represents the carboxybiotin form of the enzyme.

inability of acetyl-CoA to affect the value of the Hill coefficient was in marked contrast with its effect on the downwardly curving reciprocal plots obtained with pyruvate in the forward reaction as discussed in the preceding paper (Warren & Tipton, 1974*b*). The reciprocal plot presented in Fig. 1 was either a smooth curve or polyphasic, since careful studies at very low concentrations of oxaloacetate yielded K_m values for oxaloacetate of less than 0.7 μM. Such reciprocal plots suggest negatively co-operative interactions (Levitzki & Koshland, 1969) between oxaloacetate and pig liver pyruvate carboxylase, but more extensive studies will be needed to confirm such a postulate. It is worth noting, however, that the kinetic explanations that have been proposed to explain such reciprocal plots involving pyruvate (McClure *et al.*, 1971; Scrutton, 1971) are incapable of explaining downwardly curving reciprocal plots involving oxaloacetate.

Reaction pathway for the decarboxylation of oxaloacetate

All the results presented in this paper were entirely consistent with the reaction pathway presented in Scheme 1. The enzyme does not obey a classical double-displacement (Ping Pong) mechanism, since all interactions between the substrates and effectors (free Mg^{2+}, $MgADP^-$, P_i and oxaloacetate) yielded intersecting reciprocal plots. In the absence of products and at saturating concentrations of oxaloacetate, the rate equation will be

$$v = \frac{V}{1 + \frac{K_m^{MgADP}}{[MgADP^-]} + \frac{K_m^{P_i}}{[P_i]} + \frac{K_s^{P_i} \cdot K_m^{MgADP}}{[P_i] \cdot [MgADP^-]}\left(1 + \frac{K_s^{Mg}}{[Mg^{2+}_{free}]}\right)} \quad (1)$$

By studying the interaction between $MgADP^-$ and P_i (Figs. 2 and 3) it was possible to derive the true values for $K_m^{P_i}$ and K_m^{MgADP}. However, the K_s values for P_i and $MgADP^-$ were only apparent and:

$$\text{Apparent } K_s^{P_i} = K_s^{P_i}\left(1 + \frac{K_s^{Mg}}{[Mg^{2+}_{free}]}\right) \quad (2)$$

$$\text{Apparent } K_s^{MgADP} = K_s^{MgADP}\left(1 + \frac{K_s^{Mg}}{[Mg^{2+}_{free}]}\right) \quad (3)$$

The interaction between $MgADP^-$ and P_i (Figs. 2 and 3) was therefore studied at several concentrations of free Mg^{2+} so that a plot of apparent $K_s^{P_i}$ or K_s^{MgADP} versus $1/[Mg^{2+}_{free}]$ yielded the true K_s values for P_i, $MgADP^-$ and Mg^{2+}_{free}. These were: $K_s^{Mg} = 1.4$ mM, $K_s^{MgADP} = 0.15$ mM, $K_s^{P_i} = 12.5$ mM, $K_m^{MgADP} = 0.12$ mM, $K_m^{P_i} = 12.0$ mM.

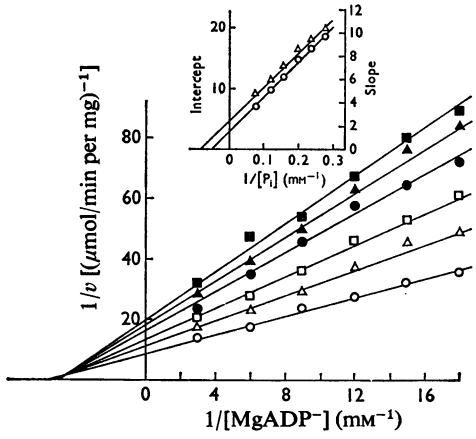

Fig. 2. *Reciprocal plot of the decarboxylation of oxaloacetate as a function of the concentration of MgADP⁻ at several fixed concentrations of P_i*

Pyruvate carboxylase (127 μg; 0.18 unit/mg) was added to the ATP-coupled assay. The P_i concentrations used were: 12.5 mM (○), 8.3 mM (△), 6.2 mM (□), 5.0 mM (●), 4.2 mM (▲), and 3.6 mM (■). Inset: the variation of the slopes (○) and intercepts (△) as a function of P_i concentration. The values of K_m^{Pi} and the apparent K_s^{Pi} calculated from these plots were 12.0 mM and 21.5 mM respectively.

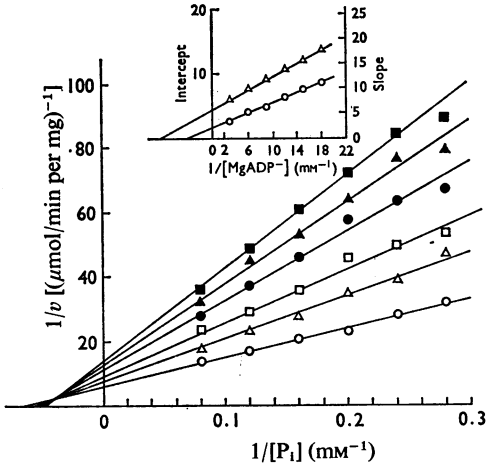

Fig. 3. *Reciprocal plot of the decarboxylation of oxaloacetate as a function of the concentration of P_i at several fixed concentrations of MgADP⁻*

The enzyme concentration and assay used were as described in Fig. 2. The MgADP⁻ concentrations used were: 0.333 mM (○), 0.167 mM (△), 0.111 mM (□), 0.083 mM (●), 0.067 mM (▲), and 0.056 mM(■). Inset: the variation of the slopes (○) and intercepts (△) as a function of MgADP⁻ concentration. The values of K_m^{MgADP} and the apparent K_s^{MgADP} calculated from these plots were 0.12 mM and 0.25 mM respectively.

The value for K_s^{Mg} of 1.4 mM is reasonably similar to that derived for the binding of free Mg^{2+} to the enzyme in the forward reaction (0.48 mM) (Warren & Tipton, 1974*b*). Similarly, K_i values in the forward reaction for MgADP⁻ (0.3 mM) and P_i (22 mM) with respect to $MgATP^{2-}$ were reasonably similar to the K_s values for these two compounds presented above. Lastly the K_s and K_m values presented above strongly suggest that the binding of P_i does not affect the binding of MgADP⁻ to the enzyme, and vice versa.

Substrate studies

Free Mg^{2+}. Eqn. 1 shows that free Mg^{2+} should exhibit rapid-equilibrium ordered kinetics with respect to both MgADP⁻ and P_i. As shown in Fig. 4, the slope replot (obtained at high concentrations of free Mg^{2+}) passed through the origin and the family of lines on the converse primary plot (Fig. 5) intersected on the $1/v$ axis. This confirmed the rapid-equilibrium ordered addition of free Mg^{2+} followed by P_i, but the reciprocal plots presented in Fig. 4 were clearly non-linear at low concentrations of free Mg^{2+} and P_i. Since the converse primary plot (Fig. 5) showed no signs of non-linearity, free Mg^{2+} must either be activating the enzyme in a co-operative manner or else the concentration of an inhibitory compound was affected by the concentration of free Mg^{2+}. The latter explanation is by far the simplest because the low value of the MgADP⁻ stability constant (1300 M^{-1}) necessitated a high concentration of ADP^{3-} at low concentrations of free Mg^{2+}. Rapid-equilibrium ordered kinetics with respect to free Mg^{2+} and MgADP⁻ were not observed because of inhibition by ADP^{3-}. The family of lines presented in Fig. 6 did not intersect on the $1/v$ axis because at any fixed concentration of free Mg^{2+}, the ratio $MgADP^-/ADP^{3-}$ was constant, even at an infinite concentration of ADP. The intercepts on the $1/v$ axis therefore reflected the degree to which the enzyme was bound to ADP^{3-}. If ADP^{3-} combined with EMg (see Scheme 1) as the only dead-end complex then eqn. (1) becomes

$$v = \frac{V}{1+\frac{K_m^{MgADP}}{[MgADP^-]}+\frac{K_m^{P_i}}{[P_i]}+\frac{K_s^{P_i}\cdot K_m^{MgADP}}{[P_i]\cdot[MgADP^-]}\left(1+\frac{K_s^{Mg}}{[Mg^{2+}_{free}]}\right)\left(1+\frac{[ADP^{3-}]}{K_i^{ADP}}\right)} \quad (4)$$

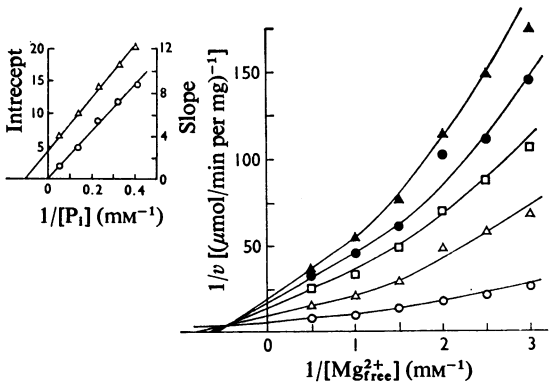

Fig. 4. *Reciprocal plot of the decarboxylation of oxaloacetate as a function of the concentration of free Mg^{2+} ions at several fixed concentrations of P_i*

Pyruvate carboxylase (81 μg; 0.18 unit/mg) was added to the ATP-coupled assay and the concentration of $MgADP^-$ was maintained at 0.4 mM. The concentrations of P_i used were: 20.0 mM (○), 7.14 mM (△), 4.35 mM (□), 3.12 mM (●) and 2.44 mM (▲). Inset: the variation of the slopes (○) and intercepts (△) as a function of P_i concentration.

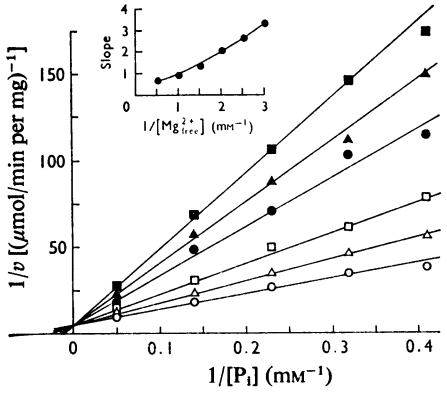

Fig. 5. *Reciprocal plot of the decarboxylation of oxaloacetate as a function of the concentration of P_i at several concentrations of free Mg^{2+} ions*

The enzyme concentration and assay were as described in Fig. 4. The free Mg^{2+} ion concentrations used were: 2.0 mM (○), 1.0 mM (△), 0.67 mM (□), 0.50 mM (●), 0.40 mM (▲) and 0.33 mM (■). Inset: the variation of the slope as a function of free Mg^{2+} ion concentration.

At infinite concentrations of $MgADP^-$ and ADP^{3-} the equation reduces to:

$$v = \frac{V}{1+\frac{K_m^{P_i}}{[P_i]}+\frac{K_s^{P_i}}{[P_i]}\cdot\frac{K_m^{MgADP}}{K_i^{ADP}}\cdot\frac{[ADP^{3-}]}{[MgADP^-]}\left(1+\frac{K_s^{Mg}}{[Mg^{2+}_{free}]}\right)} \quad (5)$$

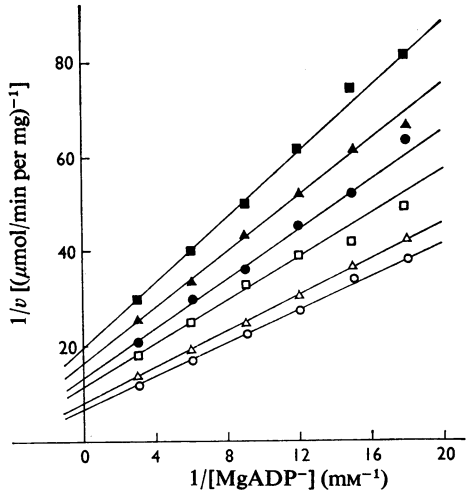

Fig. 6. *Reciprocal plot of the decarboxylation of oxaloacetate as a function of the concentration of $MgADP^-$ at several fixed concentrations of free Mg^{2+} ions*

Pyruvate carboxylase (123 μg; 0.18 unit/mg) was added to the ATP-coupled assay and the concentration of P_i was 20 mM. The concentrations of free Mg^{2+} ions used were: 2.0 mM (○), 1.0 mM (△), 0.67 mM (□), 0.50 mM (●), 0.40 mM (▲) and 0.33 mM (■).

Substituting the K_m and K_s values given above and a P_i concentration of 20 mM:

$$v = \frac{V}{1.6+\frac{0.075}{K_i^{ADP}}\cdot\frac{[ADP^{3-}]}{[MgADP^-]}\left(1+\frac{1.4}{[Mg^{2+}_{free}]}\right)} \quad (6)$$

Hence a plot of $1/v$ derived from the intercepts of Fig. 6 against

$$\frac{[ADP^{3-}]}{[MgADP^-]}\left(1+\frac{1.4}{[Mg^{2+}_{free}]}\right)$$

should yield a straight line which intersects on the abscissa at $-21.3\times K_i^{ADP}$, and as shown in Fig. 7 the value of K_i^{ADP} was 0.20 mM.

To elucidate completely the role of ADP^{3-} in the inhibition of pig liver pyruvate carboxylase the results presented in Fig. 4 were simulated on a computer. A FORTRAN program was written to simulate eqn. 4 at a fixed value of K_i^{ADP} (starting value = 0.15 mM, incremented by 0.01 mM after each run). By plotting the experimental results presented in Fig. 4 on the computer console together with the theoretical points at a fixed value of K_i^{ADP}, the latter was incremented until the best visual fit to the experimental data was obtained. This occurred when the value of K_i^{ADP} was 0.19 mM, which was in excellent agreement with the value of 0.20 mM obtained above. These results not only suggest the locus of inhibition by ADP^{3-}, but also support the reaction pathway

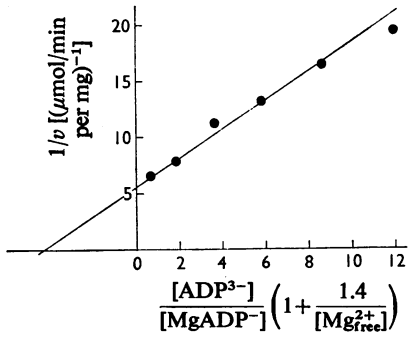

Fig. 7. *Inhibition of pyruvate carboxylase by ADP^{3-}* The value of K_i^{ADP} was determined as described in the text.

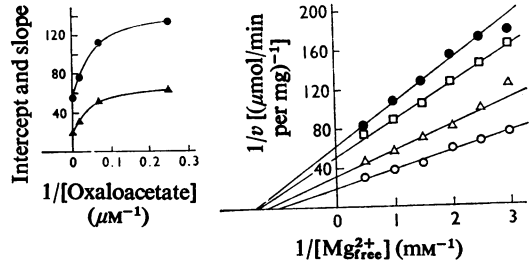

Fig. 8. *Reciprocal plot of the decarboxylation of oxaloacetate as a function of the concentration of free Mg^{2+} ions at several fixed concentrations of oxaloacetate*

Pyruvate carboxylase (52 μg; 0.17 unit/mg) was added to the ATP-coupled assay and the concentrations of P_i and $MgADP^-$ were 7.1 mM and 0.4 mM respectively. The oxaloacetate concentrations used were: 1000 μM (○), 50 μM (△), 14 μM (□) and 4 μM (●). Inset: the variation of the slopes (●) and intercepts (▲) as a function of oxaloacetate concentration.

depicted in Scheme 1. Moreover E_{ADP}^{Mg} is the predominant dead-end complex, and the absence of significant concentrations of the complex E_{ADP/P_i}^{Mg} suggests that P_i will not bind to E_{ADP}^{Mg} unless the charged P_i groups of ADP^{3-} are neutralized by nucleotide-bound Mg^{2+}.

$MgADP^-$ and P_i. The linearity of the reciprocal plots involving $MgADP^-$ and P_i (Figs. 2 and 3) suggests random-order binding in an equilibrium and not a steady-state fashion.

Oxaloacetate. Because of the non-linear nature of reciprocal plots involving this substrate it was only possible to analyse systems in which oxaloacetate was the changing fixed substrate. Reciprocal plots involving oxaloacetate and either free Mg^{2+} (Fig. 8) or $MgADP^-$ or P_i were intersecting and gave no information about the locus of binding of oxaloacetate in the reaction pathway. This information was obtained by product-inhibition studies.

Product- and dead-end-inhibition studies

These results are summarized in Table 2.

$MgATP^{2-}$. $MgATP^{2-}$ was a linear competitive product inhibitor with respect to $MgADP^-$ (Fig. 9) and P_i (Fig. 10). This confirms the random-order addition of $MgADP^-$ and P_i to EMg (see Scheme 1). At saturating concentrations of oxaloacetate the rate equation for inhibition by $MgATP^{2-}$ is

$$v = \frac{V}{1 + \frac{K_m^{MgADP}}{[MgADP^-]} + \frac{K_m^{P_i}}{[P_i]} + \frac{K_s^{P_i} \cdot K_m^{MgADP}}{[P_i] \cdot [MgADP^-]}\left(1 + \frac{K_s^{Mg}}{[Mg_{free}^{2+}]}\right)\left(1 + \frac{[MgATP^{2-}]}{K_i^{MgATP}}\right)} \quad (7)$$

The ratio of the apparent K_i^{MgADP} values determined at various concentrations of $MgADP^-$ (fixed concentration of $P_i = P_i^{MgADP}$; Fig. 9) or P_i (fixed concentration of $MgADP^- = MgADP^{P_i}$; Fig. 10) is

$$\frac{K_i^{MgATP}\,(\text{fixed } P_i)}{K_i^{MgATP}\,(\text{fixed } MgADP^-)} = \frac{\left\{K_s^{MgADP} \cdot K_m^{P_i}\left(1 + \frac{K_s^{Mg}}{[Mg_{free}^{2+}]}\right) + K_m^{MgADP} \cdot P_i^{MgADP}\right\}}{\left\{K_s^{MgADP} \cdot K_m^{P_i}\left(1 + \frac{K_s^{Mg}}{[Mg_{free}^{2+}]}\right) + K_m^{P_i} \cdot MgADP^{P_i}\right\}} \quad (8)$$

Since the concentration of Mg_{free}^{2+} was 2.0 mM in both experiments, and by using the values for the kinetic constants given above and the concentrations of the substrates given in Figs. 9 and 10, substitution in eqn. 8 gives,

$$\frac{K_i^{MgATP}\,(\text{fixed } P_i)}{K_i^{MgATP}\,(\text{fixed } MgADP^-)} = 0.47 \quad (9)$$

The experimentally observed ratio of these K_i values was 0.46 (Table 2), which is in excellent agreement with that obtained above and provides further support for the random-order addition of $MgADP^-$ and P_i. Naturally, inhibition by $MgATP^{2-}$ demanded the use of the pyruvate-coupled assay; the validity of this assay has been discussed, above, and further support was obtained by demonstrating that the inhibition of pyruvate carboxylase by adenosine, measured by the ATP-coupled assay, was competitive with respect to $MgADP^-$ (Table 2). Further, the K_i value (50 μM) was reasonably similar

Table 2. *Apparent product and dead-end inhibition constants for pig liver pyruvate carboxylase*

K_i values were determined by the method of Dixon (1953).

Product or dead-end inhibitor	Varied substrate	Observed pattern	Apparent K_i (mM)	Conditions*
$MgATP^{2-}$	$MgADP^-$	Competitive	0.25	
	P_i	Competitive	0.55	0.5 mM-$MgADP^-$
Pyruvate	$MgADP^-$	Mixed	6.0	
	P_i	Mixed	2.7	0.5 mM-$MgADP^-$
HCO_3^-	$MgADP^-$	Mixed	25	
	P_i	Non-competitive	22	
Adenosine	$MgADP^-$	Competitive	0.050	

* Other conditions as specified in the text for the assay medium.

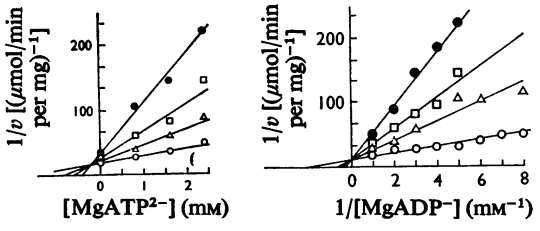

Fig. 9. *Inhibition of pyruvate carboxylase by $MgATP^{2-}$ as a function of the concentration of $MgADP^-$*

Pyruvate carboxylase (54 μg; 0.18 unit/mg) was added to the pyruvate-coupled assay. The concentrations of $MgATP^{2-}$ used were 0 (○), 0.8 mM (△), 1.6 mM (□) and 2.4 mM (●). Inset: a Dixon (1953) plot of these data. The concentrations of $MgADP^-$ were 0.20 mM (●), 0.33 mM (□), 0.50 mM (△) and 1.0 mM (○).

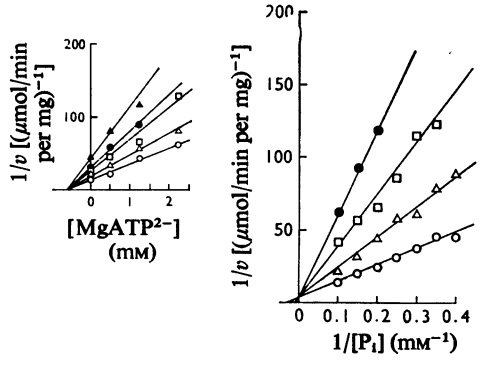

Fig. 10. *Inhibition of pyruvate carboxylase by $MgATP^{2-}$ as a function of the concentration of P_i*

Pyruvate carboxylase (100 μg; 0.16 unit/mg) was added to the pyruvate-coupled assay and the concentration of $MgADP^-$ was maintained at 0.5 mM. The concentrations of $MgATP^{2-}$ used were: 0 (○), 0.5 mM (△), 1.25 mM (□), and 2.25 mM (●). Inset: a Dixon (1953) plot of these data. The concentrations of P_i were: 2.9 mM (▲), 4.0 mM (●), 5.0 mM (□), 6.7 mM (△) and 10 mM (○).

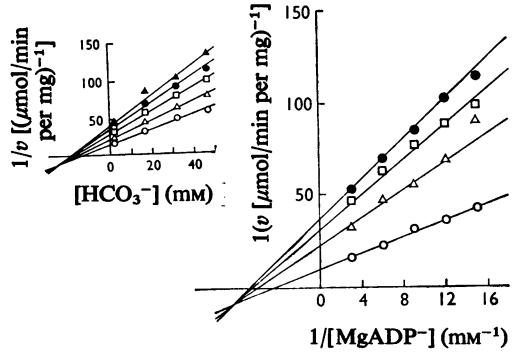

Fig. 11. *Inhibition of pyruvate carboxylase by HCO_3^- as a function of the concentration of $MgADP^-$*

Pyruvate carboxylase (92 μg; 0.18 unit/mg) was added to the ATP-coupled assay. The concentrations of HCO_3^- used were: 2 mM (○), 17 mM (△), 32 mM (□) and 47 mM (●). Inset: a Dixon (1953) plot of these data. The concentrations of $MgADP^-$ were: 0.067 mM (▲), 0.083 mM (●), 0.11 mM (□), 0.17 mM (△) and 0.33 mM (○).

to that obtained in studies of the forward reaction (90 μM; Warren & Tipton, 1974*b*).

HCO_3^-. HCO_3^- was a mixed inhibitor with respect to $MgADP^-$ (Fig. 11) and a non-competitive inhibitor with respect to P_i (Table 2). The K_i values were in the range 20–25 mM, and this was considerably higher than K_m values derived in the forward reaction (<2.5 mM). This would suggest the formation of dead-end

$$\overset{Mg}{E}\overset{HCO_3}{}$$

complexes other than EMgATP and the most likely

$$\overset{Mg}{E}\overset{HCO_3}{}$$

candidate would be $EMgADP^-/P_i$. However, since the inhibition patterns are linear (see Fig. 11) the two loci of inhibition by HCO_3^- must be separated by effectively irreversible steps. Thus the binding of oxaloacetate and the release of pyruvate probably

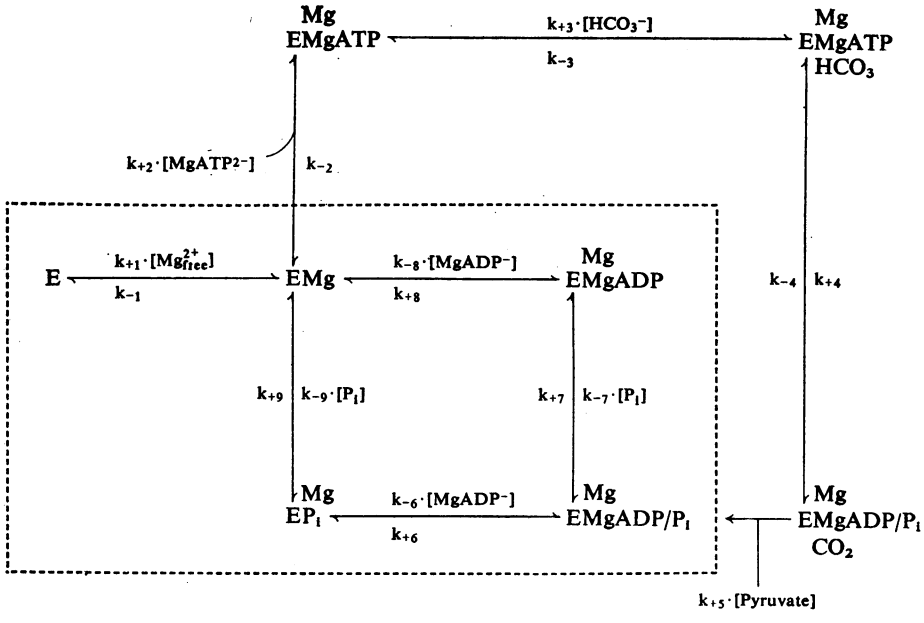

Scheme 2. *Quantitative model for the carboxylation of pyruvate by pig liver pyruvate carboxylase*

The model is described in the text. The section of the reaction mechanism enclosed by broken lines is in rapid equilibrium and may be analysed by the method of Cha (1968) so that the rate equation becomes:

$$v=\frac{V}{1+\frac{K_m^{MgATP}}{[MgATP^{2-}]}\left(1+\frac{K_s^{Mg}}{[Mg^{2+}_{free}]}\right)+\frac{K_m^{HCO_3^-}}{[HCO_3^-]}+\frac{K_m^{Pyr}}{[pyruvate]}+\frac{K_s^{MgATP}\cdot K_m^{HCO_3^-}}{[MgATP^{2-}]\cdot[HCO_3^-]}\left(1+\frac{K_s^{Mg}}{[Mg^{2+}_{free}]}\right)+\frac{K_s^{HCO_3^-}\cdot K_{Pyr}}{[HCO_3^-]\cdot[pyruvate]}}$$
$$+\frac{K_s^{MgATP}\cdot K_s^{HCO_3^-}\cdot K_{Pyr}}{[MgATP^{2-}]\cdot[HCO_3^-]\cdot[pyruvate]}\left(1+\frac{K_s^{Mg}}{[Mg^{2+}_{free}]}\right)+\frac{[MgADP^-]\cdot K_m^{MgATP}}{K_i^{MgADP}\cdot[MgATP^{2-}]}+\frac{[MgADP^-]\cdot K_s^{MgATP}\cdot K_m^{HCO_3^-}}{K_i^{MgADP}\cdot[MgATP^{2-}]\cdot[HCO_3^-]}$$
$$+\frac{[MgADP^-]\cdot K_s^{MgATP}\cdot K_s^{HCO_3^-}\cdot K_{Pyr}}{K_i^{MgADP}\cdot[MgATP^{2-}]\cdot[HCO_3^-]\cdot[pyruvate]}+\frac{[P_i]\cdot K_m^{MgATP}}{K_i^{Pi}\cdot[MgATP^{2-}]}+\frac{[P_i]\cdot K_s^{MgATP}\cdot K_m^{HCO_3^-}}{K_i^{Pi}\cdot[MgATP^{2-}]\cdot[HCO_3^-]}$$
$$+\frac{[P_i]\cdot K_s^{MgATP}\cdot K_s^{HCO_3^-}\cdot K_{Pyr}}{K_i^{Pi}\cdot[MgATP^{2-}]\cdot[HCO_3^-]\cdot[pyruvate]}+\frac{[MgADP^-]\cdot[P_i]\cdot K_m^{MgATP}}{K_i^{MgADP}\cdot K_i^{Pi}\cdot[MgATP^{2-}]}+\frac{[MgADP^-]\cdot[P_i]\cdot K_s^{MgATP}\cdot K_m^{HCO_3^-}}{K_i^{MgADP}\cdot K_i^{Pi}\cdot[MgATP^{2-}]\cdot[HCO_3^-]}$$
$$+\frac{[MgADP^-]\cdot[P_i]\cdot K_s^{MgATP}\cdot K_s^{HCO_3^-}\cdot K_{Pyr}}{K_i^{MgADP}\cdot K_i^{Pi}\cdot[MgATP^{2-}]\cdot[HCO_3^-]\cdot[pyruvate]}$$

where:

$$K_s^{Mg}=\frac{k_{-1}}{k_{+1}}=0.96\,\text{mM};$$

$$K_m^{MgATP}=\frac{k_{+4}}{k_{+2}}=0.18\,\text{mM};\quad K_s^{MgATP}=\frac{k_{-2}}{k_{+2}}=0.34\,\text{mM};$$

$$K_m^{HCO_3^-}=\frac{(k_{+4}+k_{-3})}{k_{+3}}=1.0\,\text{mM};\quad K_s^{HCO_3^-}=\frac{k_{-3}}{k_{+3}}=0.8\,\text{mM};$$

$$K_m^{Pyr}=\frac{(k_{+4}+k_{-4})}{k_{+5}}=0.22\,\text{mM};\quad K_{Pyr}=\frac{k_{-4}}{k_{+5}}=0.33\,\text{mM};$$

$$K_i^{MgADP}=\frac{k_{+8}}{k_{-8}}=\frac{k_{+6}}{k_{-6}}=0.14\,\text{mM};$$

$$K_i^{Pi}=\frac{k_{+9}}{k_{-9}}=\frac{k_{+7}}{k_{-7}}=12.0\,\text{mM};\ \text{and}$$

$$V=k_{+4}\cdot E_{total}$$

take place after the binding of free Mg^{2+}, $MgADP^-$ and P_i.

Pyruvate. This was a mixed inhibitor with respect to both $MgADP^-$ and P_i (Table 2). Unfortunately, the non-linear nature of reciprocal plots involving oxaloacetate precluded an investigation into the interaction of pyruvate with this substrate. The Theorell–Chance mechanism depicted in Scheme 1 is only supported by analogy with the forward reaction discussed in the preceding paper (Warren & Tipton, 1974*b*) and the results obtained with the chicken liver enzyme (Barden *et al.*, 1972).

Discussion

The results presented above and in the preceding paper (Warren & Tipton, 1974*b*) are entirely consistent with each other. However, pyruvate carboxylase is a multisubstrate, multieffector enzyme and too few kinetic experiments have been performed to permit precise quantitative values for the individual kinetic constants. The values may be derived, however, to a first approximation, for the model depicted in Scheme 2, which has been constructed with the physiological role of pyruvate carboxylase in mind. The model is valid at pH 8.0, 30°C, an ionic strength of 150–200mM and in the presence of saturating concentrations of K^+ ions and acetyl-CoA. Although the concentration of K^+ is likely to be saturating *in vivo* this is unlikely to be true for acetyl-CoA. The model depicts the forward reaction of pyruvate carboxylase, and irreversibility has been depicted by the effective absence of oxaloacetate, since this compound is present in the mitochondrial matrix in very low concentrations (see Gumaa *et al.*, 1971). This also eliminates the need to consider the non-linear reciprocal plots obtained with this compound.

The model depicted in Scheme 2 could form the basis of an attempt to understand the regulatory properties of pyruvate carboxylase *in vivo*. In this context the most important step would be to quantify the role of acetyl-CoA in the reaction mechanism. Re-evaluation of the kinetic constants to conform with the conditions which probably exist in the liver cell [pH 7.2 (Walker *et al.*, 1969), an ionic strength of 250mM (Hohorst, 1960, as quoted by Williamson *et al.*, 1967) and a temperature of 37°C] should not prove too difficult, although the possibility of mechanistic changes in the reaction mechanism (McClure & Lardy, 1971) must be taken into consideration. Moreover, the information about the locus of action of nucleotides capable of inhibiting pyruvate carboxylase should prove useful at physiological pH values, where the concentrations of these compounds will be much higher. Subject to the possible complications of applying results obtained *in vitro* to the conditions that exist *in vivo*. (Sols & Marco, 1970), such a model could help to verify and possibly extend control systems that have been postulated for this enzyme (see McClure & Lardy, 1971, for references).

We thank the Medical Research Council for a studentship (to G. B. W.).

References

Barden, R. E., Fung, C. H., Utter, M. F. & Scrutton, M. C. (1972) *J. Biol. Chem.* **247**, 1323–1333
Cha, S. (1968) *J. Biol. Chem.* **243**, 820–825
Dixon, M. (1953) *Biochem. J.* **55**, 170–171
Florini, J. R. & Vestling, C. S. (1957) *Biochim. Biophys. Acta* **25**, 575–578
Gumaa, K. A., McLean, P. & Greenbaum, A. L. (1971) *Essays in Biochemistry* **7**, 39–86
Levitzki, A. & Koshland, D. E. (1969) *Proc. Nat. Acad. Sci. U.S.* **62**, 1121–1128
Lineweaver, H. & Burk, D. (1934) *J. Amer. Chem. Soc.* **56**, 658–666
McClure, W. R. (1969) *Biochemistry* **8**, 2782–2786
McClure, W. R. & Lardy, H. A. (1971) *J. Biol. Chem.* **246**, 3591–3596
McClure, W. R., Lardy, H. A., Wagner, M. & Cleland, W. W. (1971) *J. Biol. Chem.* **246**, 3579–3583
Moss, J. & Lane, M. D. (1972) *J. Biol. Chem.* **247**, 4952–4959
Scrutton, M. C. (1971) *Metabolism* **20**, 168–186
Scrutton, M. C. & Mildvan, A. S. (1968) *Biochemistry* **7**, 1490–1505
Sols, A. & Marco, R. (1970) *Curr. Top. Cell Regul.* **2**, 227–273
Walker, W. D., Goodwin, F. J. & Cohen, R. D. (1969) *Clin. Sci.* **36**, 409–417
Warren, G. B. & Tipton, K. F. (1974*a*) *Biochem. J.* **139**, 297–310
Warren, G. B. & Tipton, K. F. (1974*b*) *Biochem. J.* **139**, 311–320
Williamson, D. H., Lund, P. & Krebs, H. A. (1967) *Biochem. J.* **103**, 514–527